Title	Performance analysis of one-source-with-one-helper transmission over shadowed κ-μ fading multiple access channels
Author(s)	Qian, Shen; He, Jiguang; Zhou, Xiaobo; Imai, Takamasa; Matrumoto, Tad
Citation	IET Communications: 1-13
Issue Date	2022-05-06
Type	Journal Article
Text version	publisher
URL	http://hdl.handle.net/10119/17757
Rights	
Description	

IET Communications

IET The Institution of Engineering and Technology WILEY

ORIGINAL RESEARCH

Performance analysis of one-source-with-one-helper transmission over shadowed κ-μ fading multiple access channels

Shen Qian[1] | **Jiguang He**[2,3] | **Xiaobo Zhou**[4] | **Takamasa Imai**[1] | **Tad Matrumoto**[5]

[1]Department of Information Systems Creation, Faculty of Engineering, Kanagawa University, Yokohama, Japan

[2]Technology Innovation Institute, Abu Dhabi, United Arab Emirates

[3]Centre for Wireless Communications, University of Oulu, Oulu, Finland

[4]School of Computer Science and Technology, Tianjin University, Tianjin, China

[5]IMT Atlantique, Brest, France

Correspondence
Shen Qian, Department of Information Systems Creation, Faculty of Engineering, Kanagawa University, Yokohama, Japan.
Email: shenqian@kanagawa-u.ac.jp

Abstract
The performance of correlated sources transmission over multiple access shadowed κ-μ fading channels is investigated, in which one of the correlated sources needs to be recovered at the destination, whereas the other serves as a helper. The sufficient condition for lossless coding is determined by the intersection of the modified Slepian–Wolf region and the multiple access channel region. The outage probability upper bounds are derived based on the sufficient condition, with the Gaussian codebook capacity and the constellation constrained capacity, respectively. The difference between the outage probabilities derived with the two kinds of capacities is found to be very minor, when the spectrum efficiency or source rate is low; however, with high spectrum efficiency or high source rate, such difference becomes significant. A closed-form outage approximation is also obtained at the high signal-to-noise ratio region. The accuracy of the analytical results is verified by the Monte-Carlo simulations. It is found that shadowing significantly affects the outage performance, however, it has no effect on the diversity gain. Furthermore, the power allocation between the source and the helper is studied to minimize the outage probability and it is found that generally more power should be allocated to the helper in the case with higher source-helper correlation.

1 | INTRODUCTION

With the commercialization of the fifth-generation (5G) network, wireless sensor networks (WSNs) play a vital role in the Internet of Things (IoT) [1], and they are also considered as a promising candidate in the deployment of 6G network [2]. The application of WSNs in IoT provides us many advantages such as city safety, disaster prevention and management, and smart agriculture.

One of the important advantages of WSNs in monitoring is their cooperative effort. A large number of sensor nodes are deployed to collect the data and report it to the fusion center [3]. The information collected by these sensor devices is correlated spatially and/or temporally, and therefore, the data rates of lossless coding for all sensor nodes are determined by the Slepian–Wolf theorem. An asynchronous Slepian–Wolf coding, in which each encoder samples a source sequence with a certain delay, was investigated in [4] and the achievable rate region was found not always coincide with that of the synchronous Slepian–Wolf

coding system without any delay. However, in cooperative communication systems, correlated data sequences are transmitted from the source and the relay to the destination, the destination aims only to recover the information sent from the source. This system setup does not perfectly match the Slepian–Wolf theorem which intends to recover the two correlated sources at the destination, whereas, the admissible rate region for the source and relay is accurately determined by the theorem for source coding with side information [5].

Compared with the orthogonal transmission, non-orthogonal transmission over multiple access channel (MAC) has high transmission efficiency and hence improves the throughput and reduces latency significantly [6]. In WSNs with MAC transmission, sensors collect the data and transmit it to the fusion center simultaneously. However, a general necessary and sufficient condition for lossless coding of correlated sources over a MAC is still an open question. The admissible rate region of transmitting multiple correlated binary sources over a Gaussian MAC was derived in [7]. In [8], the sufficient

conditions and necessary conditions for the achievability of a certain distortion pair with Gaussian sources over a MAC with unidirectional conferencing encoders were presented, expressing the distortion pairs as a function of the channel signal-to-noise ratio (SNR) and of the source correlation. Padakandla characterized a set of sufficient conditions of transmitting two distributed correlated sources over MAC and interference channels [9], and extended to the performance analysis of joint source-channel decoding [10].

Zhou et al. [11] determined the sufficient condition for correlated sources coding over a quasi-static Rayleigh fading multiple access channel (MAC), considering the sufficient condition for the successful transmissions is that the Slepian–Wolf and MAC regions intersect. He et al. [12] calculated the outage probability of independent binary sources over a non-orthogonal multiple access relay channel, depending on the sufficient condition of lossless communication over MAC using a helper. Furthermore, Song et al. [13] extended the work of Zhou et al. [11] to the case where only one of the sources needs to be recovered at the destination, whereas the other source serves as a helper. Motivated by decision-making systems, where the aim is to make right decisions based on the observations, an approximated, yet accurate, Wyner-Ziv rate region was propose in [14], allowing distortion in wireless transmission. However, Rayleigh fading with non-line-of-sight components only was assumed in [11–14], and the shadowing during the transmission was ignored.

In the emerging IoT applications, such as surveillance networks or smart agriculture, both line-of-sight (LOS) and non-LOS components co-exist in device-to-device (D2D) communications links, because of the features of mobile device behaviour. Furthermore, as mobile devices are blocked by obstacles such as buildings or vegetation, these links will also be heavily susceptible to possible deep fading caused by shadowing [15, 16]. To the best of the authors' knowledge, the outage analysis of the correlated sources transmission in shadowed fading with the coexistence of both LOS and non-LOS components has yet to be reported in the literature.

Paris [17] introduced shadowing into κ-μ fading model, a generalized multipath model proposed by Yacoub [18], assuming that the dominant components of all the clusters are subject to random fluctuations. Since the shadowed κ-μ fading is a versatile model which is applicable to various scenarios, such as, channel models for land mobile satellite communications, underwater acoustic communications, body-centric fading communications, and D2D communications [19, 20], it invokes emerging and growing interest in the κ-μ channel model's applicability to shadowed fading. The utilization of the shadowed κ-μ model for characterizing signal reception in D2D communications was validated through field measurements [15]. Bhatnagar [21] characterized the correlated shadowed κ-μ fading model, in terms of probability density function (PDF) and moment generating function. Zhang et al. derived the exact and asymptotic expressions of higher-order statistics in low- and high-SNR regimes with shadowed κ-μ fading channels [22]. The effective rate of MISO systems over independent and identically shadowed κ-μ fading channels was derived in [23]. The ergodic capacities and the outage probabilities of of two-user NOMA

system over shadowed κ-μ fading channels were derived in [24]. Yang et al. [25] investigated performance of a power-beacon-assisted multi-input multi-output wireless communication network, assuming that the wireless power transfer link follows the shadowed κ-μ distribution whereas the information transmission link follows the Rayleigh distribution.

The main objective of this paper is to fill the blanks in [11–14] and to theoretically investigate outage probability of correlated source transmission [13], where all the links are assumed to experience a non-homogeneous practical wireless block fading channel delineated by shadowed κ-μ fading [17]. As only one of the correlated sources needs to be recovered losslessly at the destination, the scheme is referred to as one-source-with-one-helper transmission over a fading MAC, with the modified Slepian–Wolf region being defined to determine the admissible rate for source coding. Moreover, in [11–14], Gaussian codebook capacity (GCC) was assumed for describing the relationship between the coding rate and the blockwise instantaneous SNR. However, in practice, instantaneous channel capacity is constrained by specific modulation constellation size, known as the constellation constrained capacity (CCC) [26]. Therefore, it is more reasonable to evaluate the performance of practical systems assuming the transmit symbols are from a finite alphabet set with constellation constrained capacity.

This study contributes to the following areas:

- The outage probability upper bound for the one-source-with-one-helper transmission over shadowed κ-μ fading channels is derived. The sufficient condition for lossless coding is determined by the intersection of the modified Slepian–Wolf region and the MAC region, assuming that the source-channel separation theorem holds. Furthermore, the explicit, yet accurate closed-form outage probability expression is obtained, by approximating the PDF and cumulative distribution function (CDF) of shadowed κ-μ fading in the high SNR region. The accuracy of the approximation and the outage probabilities are verified using the analytical results and Monte-Carlo simulations, respectively. The numerical results indicate that the shadowing significantly affects the outage performance, however, has no impact on the diversity gain.
- The outage probability of the one-source-with-one-helper transmission over MAC with GCC and that with CCC is derived, respectively. The numerical results indicate that the difference between the GCC- and CCC- based outage probabilities is negligible with low spectrum efficiency or low source rate. In contrast, the difference becomes significant when the spectrum efficiency or the source rate becomes high. The effect of shadowing, source-helper correlation, spectrum efficiency and source rate, the number of multipath clusters, and the dominant components of the clusters on the outage performance is investigated.
- Optimal power allocation, under the total transmit power constraint, between the source and the helper is also investigated to achieve the lowest outage probability. With higher source-helper correlation, the more power should be allocated to the helper for the considered system. However, with a large dominant component power ratio in the
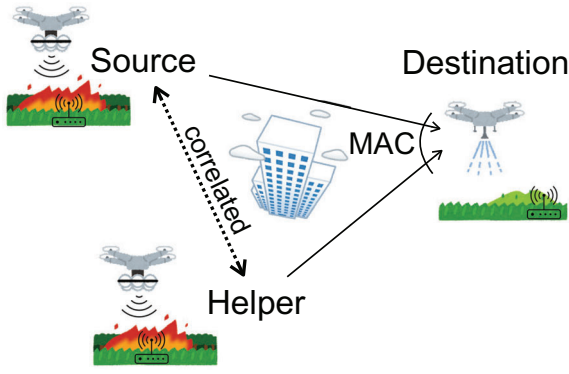
FIGURE 1 An one-source-with-one-helper transmission system over MAC

FIGURE 2 Abstract model for encoding and decoding of the one-source-with-one-helper transmission over MAC

TABLE 1 Length and rates of information sequences

	S and H	U_1 and U_2	X_1 and X_2
Length	k	ℓ	n
Source rate	$R^s = \frac{\ell}{k}$		
Spectrum efficiency		$R^c = \frac{\ell}{n}$	
Total coding efficiency	$\acute{R} = \frac{k}{n}$		

helper-destination channel, it is more effective to assign more power to the source to achieve a lower outage probability.

The remainder of the paper is organized as follows: Section 2 describes the system model for analysing the one-source-with-one-helper transmission over fading MAC. Section 3 introduces the definition of the admissible rate region, derivation of outage probability, and the asymptotic tendency analyses. Section 4 exhibits the numerical results of the outage probability with accuracy being verified by Monte-Carlo simulations. Finally, Section 5 concludes the paper with some concluding remarks.

2 | SYSTEM MODEL

2.1 | Non-orthogonal MAC transmission

We consider a simple, one-source-with-one-helper system, as shown in Figure 1. One source, S communicates with the common destination D with the help of H. The information sequences of the S and H are correlated since they are gathered from the sensors monitoring the same scenario. Non-orthogonal MAC is assumed for cooperative transmission. Therefore, the information of S and H is transmitted to D simultaneously within one time slot.

D performs the joint decoding process by utilizing the correlation between S and H once it receives the signal from the source and the helper. We concentrate only on the recovery of the source information sequence of S.

2.2 | Coding model

Let the binary source S be stationary, memoryless, and be drawn from a binary set $(\Omega = \{0, 1\})$ according to a Bernoulli$(\frac{1}{2})$ distribution and hence, $\Pr(S = 1) = \Pr(H = 1) = \frac{1}{2}$. The correlation between S and H is described, assuming H takes value from the output of a binary symmetric channel (BSC), with S being the channel input, as in [27]. The complementary parameter of the BSC channel is denoted by p, which also represents the correlation between S and H. More specifically, p indicates the bit flipping probability between S and H, as $S = H \oplus E$, where
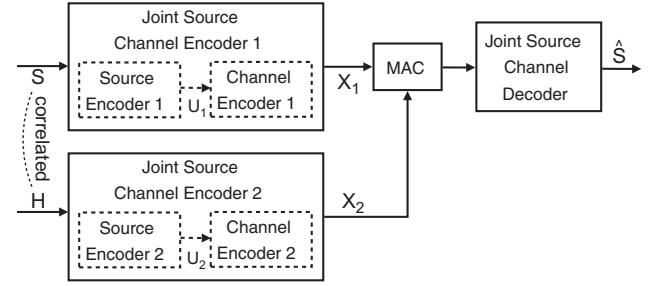
$\oplus$ denotes the modulo-2 addition and the binary random variable E satisfies $\Pr(E = 1) = p$.

As shown in Figure 2, S and H are first encoded by their own source encoders, respectively, to representation patterns U_1 and U_2, which are then encoded to signal sequences X_1 and X_2 for transmitting to D. Table 1 shows the length of information sequences before and after the source and channel encoding. In general, the normalized source rate R^s is smaller than 1 because the redundancy in the length-ℓ codewords is to be removed. R^c is the normalized spectrum efficiency including the channel coding rate and the modulation order multiplicity of the corresponding channel [28]. R^c is greater than 1, as on the contrary redundancy is added to the information sequence (i.e., the output of source encoder) for reliable communications. The total rate of the joint source-channel coding $\acute{R}$ is defined as

$$\acute{R} = \frac{R^c}{R^s}. \tag{1}$$

In the above equation, we assume that Shannon's lossless source-channel separation holds. Note that $\acute{R}$ takes an arbitrary value greater than 0. At the destination, an iterative joint decoding fashion is considered to retrieve S using the source-helper correlation.

2.3 | Channel model

Since MAC is assumed in the transmission, the signal received at D, $y_D[n]$, is expressed as

$$y_D[n] = \sqrt{P_1}h_1 x_1[n] + \sqrt{P_2}h_2 x_2[n] + n_D[n], \tag{2}$$

respectively, where n indicates the symbol indices, and P_i ($i \in \{1, 2\}$) is the transmit power of the corresponding node. The

geometric gain of each link related to the transmission distance is normalized to unity in this discussion. $x_1[n]$ and $x_2[n]$ denote the modulated symbols corresponding to the coded information sequences, transmitted from S and H, respectively. h_i ($i \in \{1, 2\}$) denotes the complex channel gain, and n_D is zero-mean additive white Gaussian noise (AWGN) with the variance of $N_0/2$ per dimension. It is assumed that $\mathbb{E}[|h_i|^2] = 1$ and h_i stays constant over one block duration due to the block fading assumption.

The average and instantaneous SNRs are expressed as $\bar{\gamma}_i = P_i \frac{E_s}{N_0}$ and $\gamma_i = |h_i|^2 \bar{\gamma}_i$, where ($i \in \{1, 2\}$), respectively, with E_s being the transmit power of each symbol. The variations due to shadowing is taken into account since κ-μ shadowing fading is considered.

We also assume that the S-D and H-D links suffer from shadowed κ-μ fading. The PDF of instantaneous SNR with the shadowed κ-μ channel is given by [29]

$$f_{\kappa\mu}(\gamma_i) = \frac{\mu^\mu m^m (1+\kappa)^\mu}{\Gamma(\mu)\bar{\gamma}_i(\mu\kappa+m)^m} \left(\frac{\gamma_i}{\bar{\gamma}_i}\right)^{\mu-1} \exp\left(-\frac{\mu(1+\kappa)\gamma_i}{\bar{\gamma}_i}\right)$$

$$\times {}_1F_1\left(m, \mu; \frac{\mu^2\kappa(1+\kappa)\gamma_i}{(\mu\kappa+\mu)\bar{\gamma}_i}\right), \ (i \in \{1, 2\}), \quad (3)$$

where ${}_1F_1(\cdot)$ and $\Gamma(\cdot)$ are the confluent hypergeometric function[30, Section 9.210] and Gamma function, respectively. By normalizing the noise variance to unity, the average SNR $\bar{\gamma}$ is equivalent to the average received power.

We assume LOS shadowed fading where shadowing is introduced in multipath fading by assuming that the dominant component is subject to random variation [17]. Therefore, the parameter $m(m \geq 0)$ in (3) and (4) denotes the shadowing severity, where $m = 0$ indicates complete shadowing and $m \to \infty$ corresponds to no shadowing in the resultant dominant component. κ denotes the ratio between the power of the dominant component to the total power of the scattered components, and μ is the number of multipath clusters. Usually, μ is a natural number. However, it can be extended to a non-negative real number as noted in [18].

The CDF of γ_i with shadowed κ-μ fading is given by

$$F_{\kappa\mu}(\gamma_i) = \frac{\mu^{\mu-1} m^m (1+\kappa)^\mu)}{\Gamma(\mu)(\mu\kappa+m)^m} \left(\frac{1}{\bar{\gamma}_i}\right)^\mu$$

$$\times \Phi_2\left(\mu - m, m; \mu + 1; \frac{-\mu(1+\kappa)\gamma_i}{\bar{\gamma}_i},\right.$$

$$\times \left.\frac{-\mu(1+\kappa)m\gamma_i}{\bar{\gamma}_i(\mu\kappa+m)}\right), \quad (4)$$

where $\Phi_2(\cdot)$ is the bivariate confluent hypergeometric function.

By specializing the parameters m, κ, and μ in (3) and (4), some typical fading models, that is, one-side Gaussian, Rayleigh, Nakagami-m, Rician, κ-μ, and Rician can be obtained from the κ-μ shadowed fading [17, 31], shown in Table 2. K and m_N

TABLE 2 Typical fading models related to the κ-μ shadowed fading

Fading model	m	κ	μ
Rayleigh	–	0	1
Rician	∞	K	1
Nakagami-m	–	0	m_N
κ-μ	∞	κ	μ
One-sided Gaussian	∞	0	0.5

in Table 2 stand for K factor and shape factor in Rician and Nakagami-m fading, respectively.

3 | OUTAGE PROBABILITY ANALYSES

3.1 | Admissible rate regions

According to Shannon's source-channel separation theorem [5], since the source coding is independent from the channel characteristics and the channel coding is independent from the distribution of the source, the joint source-channel coding for X_1 and X_2 can be separated into a two-stage scheme: MAC description and distributed source coding.

The achievable capacity region of the MAC, $\mathbb{R}^{\text{MAC}}$, is defined as a closure of the convex hull of the rate pair (R_1^c and R_2^c) satisfying

$$\begin{cases} R_1^c \leq C(\gamma_1), \\ R_2^c \leq C(\gamma_2), \\ R_1^c + R_2^c \leq C(\gamma_1 + \gamma_2), \end{cases} \quad (5)$$

where $C(\gamma_i) = \log_2(1 + \gamma_i)$ ($i \in \{1, 2\}$) is the channel capacity with the instantaneous SNR γ_i. Dividing both sides of (5) with $\dot{R}$ according to source-channel separation theorem, we obtain

$$\begin{cases} R_1^s = \frac{R_1^c}{\dot{R}} \leq \frac{C(\gamma_1)}{\dot{R}}, \\ R_2^s = \frac{R_2^c}{\dot{R}} \leq \frac{C(\gamma_2)}{\dot{R}}, \\ R_1^s + R_2^s \leq \frac{C(\gamma_1+\gamma_2)}{\dot{R}}. \end{cases} \quad (6)$$

The region is illustrated as a bounded pentagonal, as shown in Figure 3. For the sake of brevity, we assume that $\dot{R} = \dot{R}_1 = \dot{R}_2$, where $\dot{R}_1 = \frac{R_1^c}{R_1^s}$ and $\dot{R}_2 = \frac{R_2^c}{R_2^s}$.

For the lossless distributed source coding problem, according to the Slepian–Wolf theorem[32], the rate pair (R_1^s and R_1^s) must satisfy the following inequalities:

$$\begin{cases} R_1^s \geq H(\text{S}|\text{H}), \\ R_2^s \geq H(\text{H}|\text{S}), \\ R_1^s + R_2^s \geq H(\text{S}, \text{H}), \end{cases} \quad (7)$$
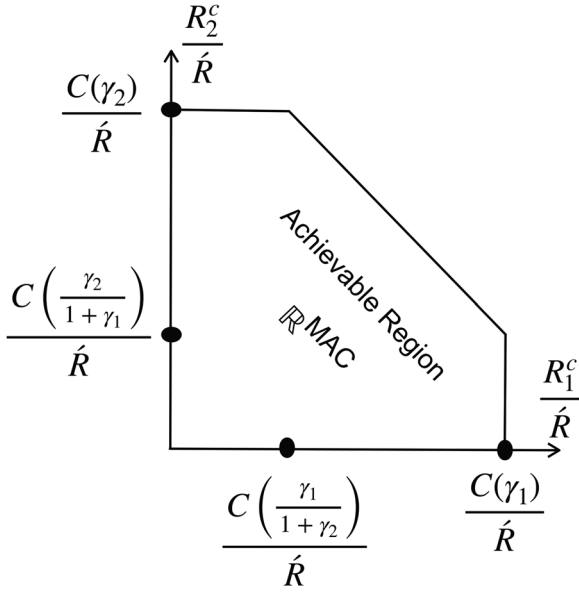
FIGURE 3 Achievable region $\mathbb{R}^{\text{MAC}}$ of MAC transmission
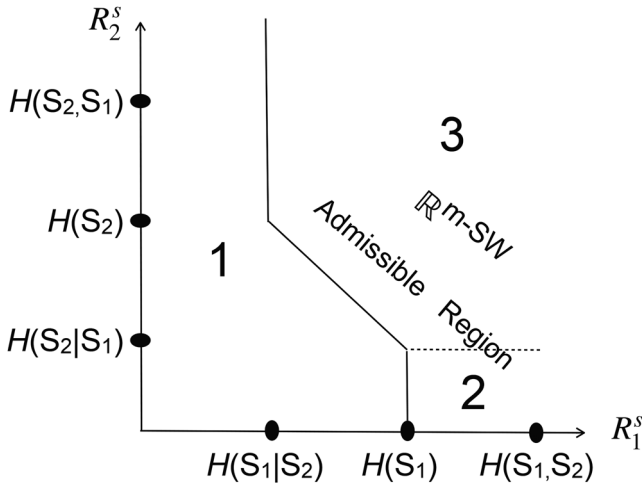

FIGURE 4 Admissible region $\mathbb{R}^{\text{m−SW}}$ specified with Slepian–Wolf theorem

where $H(\cdot|\cdot)$ and $H(\cdot,\cdot)$ denote the conditional and the joint entropy, respectively. If the rate pair (R_1^s and R_2^s) falls outside the admissible region as shown in Figure 4, which can be divided into two areas 1 and 2, the decoder cannot guarantee the reconstruction of S and H with arbitrarily small error probability. Since S and H follow Bernoulli($\frac{1}{2}$) distribution and H is the flipped version of S, we have $H(S) = H(H) = 1$, $H(S|H) = H(H|S) = H(p)$, and $H(S,H) = H(H) + H(S|H) = H(S) + H(H|S) = 1 + H(p)$, where $H(p) = -p\log_2(p) - (1-p)\log_2(1-p)$ is the binary entropy function.

Since we consider only the case where only S needs to be recovered at the destination, area 2 in Figure 4 is also part of the admissible rate region. Hence, the inequalities in (7) are rewrit-

ten as

$$
R_1^s \geq \begin{cases} H(S|H), & \text{for} \quad H(H) \leq R_2^s \\ H(H,S) - R_2^s, & \text{for} \quad H(H|S) \leq R_2^s \leq H(H) \quad (8) \\ H(S), & \text{for} \quad 0 \leq R_2^s \leq H(S|H), \end{cases}
$$

which is referred to as the modified Slepian–Wolf region $\mathbb{R}^{\text{m−SW}}$.

Even though the accurate admissible rate region for one-source-with-one-helper transmission is determined by the source coding with side information theorem, the Slepian–Wolf theorem can replace the source coding with side information theorem as a linear approximation, without losing the accuracy for calculating the outage probability, as shown in [33]. Therefore, the analytical results in this work are regarded as upper bounds for the performance of the practical signalling schemes.

Then, the sufficient conditions for lossless coding of S and H over MAC can be written as

$$
\begin{cases} H(S|H) \leq R_1^s \leq \frac{C(\gamma_1)}{\acute{R}}, \\ H(H|S) \leq R_2^s \leq \frac{C(\gamma_2)}{\acute{R}}, \\ H(S,H) \leq (R_1^s + R_2^s) \leq \frac{C(\gamma_1+\gamma_2)}{(\acute{R}}, \end{cases} \quad (9)
$$

by a joint consideration of MAC rate region defined in (5) and modified Slepian–Wolf region defined in (8). The above equation indicates that $\mathbb{R}^{\text{MAC}}$ and $\mathbb{R}^{\text{m−SW}}$ should intersect with each other to guarantee the success of the one-source-with-one-helper transmission over MAC.

Since the source-channel separation theorem holds for point-to-point transmission and is not optimal in general, (9) is only the sufficient but not necessary condition for transmitting one source with one helper over a MAC with arbitrary small error probability. This also leads to that the derived expression is the upper bound of outage probability as in [34].

3.2 | Outage probability calculation

For an outage event, D cannot guarantee the reconstruction of S with an arbitrarily small error probability when $\mathbb{R}^{\text{MAC}}$ and $\mathbb{R}^{\text{m−SW}}$ do not have an intersection, that is, $\mathbb{R}^{\text{MAC}} \cap \mathbb{R}^{\text{m−SW}} =$. The outage event can be divided into two cases:

$$
\text{case 1}: \frac{C(\gamma_1)}{\acute{R}} < H(S|H) \text{ and case 2}: \frac{C(\gamma_1)}{\acute{R}} \geq H(S|H),
$$

$$(10)$$

as shown in Figures 5 and 6, respectively. In case 1, since $\frac{C(\gamma_1)}{\acute{R}}$ is smaller than $H(S|H)$, the outage always happens regardless of the value of $\frac{C(\gamma_2)}{\acute{R}}$. However, in case 2, the outage occurs only if $\frac{C(\gamma_1+\gamma_2)}{\acute{R}} < H(S,H)$. Since $\frac{C(\gamma_1)}{\acute{R}} < H(S|H)$ and $\frac{C(\gamma_1)}{\acute{R}} \geq H(S|H)$ are distinctive, the outage probability P^{out} of the
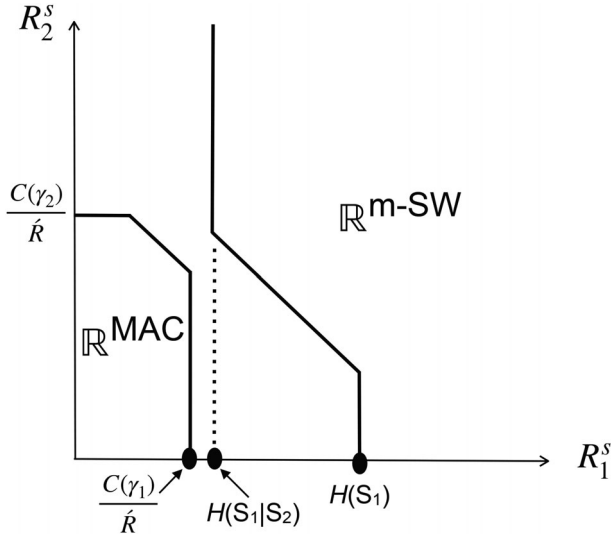
FIGURE 5 Outage case 1, when $\frac{C(\gamma_1)}{\acute{R}} < H(S|H)$
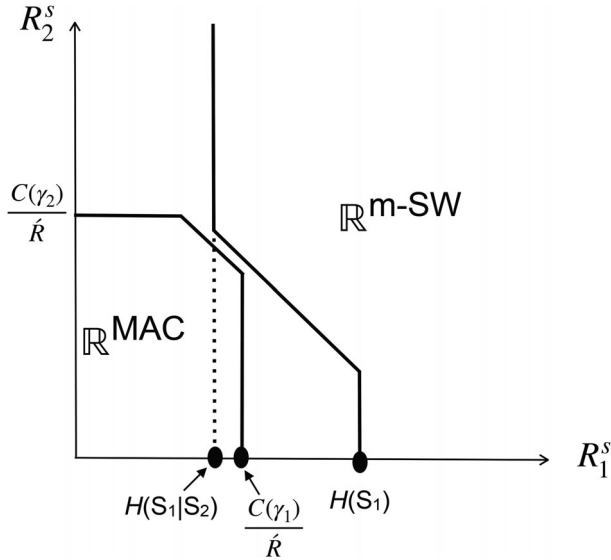

FIGURE 6 Outage case 2, when $\frac{C(\gamma_1)}{\acute{R}} \geq H(S|H)$

one-source-with-one-helper transmission over MAC is expressed as

$$P^{out} = P^{out}_{case1} + P^{out}_{case2}, \qquad (11)$$

where

$$P^{out}_{case1} = Pr\left\{ \frac{C(\gamma_1)}{\acute{R}} < H(S|H), \frac{C(\gamma_2)}{\acute{R}} \geq 0 \right\}, \qquad (12)$$

and

$$P^{out}_{case2} = Pr\left\{ H(S|H) \leq \frac{C(\gamma_1)}{\acute{R}} \leq H(S), \right.$$
$$\left. \times \frac{C(\gamma_1 + \gamma_2)}{\acute{R}} \leq H(S,H) \right\}. \qquad (13)$$

3.3 | Outage derivation with GCC

With the assumption that Gaussian code book is used, the relationship between the instantaneous channel SNR γ_1 ($i \in \{1, 2\}$) and the rate $\acute{R}$ is written as

$$\acute{R} \times H(S) = \log_2(1 + \gamma_1), \qquad (14)$$

$$\acute{R} \times H(H) = \log_2(1 + \gamma_2). \qquad (15)$$

Then, with the assumption that each link experiences statistically independent block κ-μ shadowed fading, the outage probability is written as

$$P^{out}_{case1} = Pr\left\{ \frac{C(\gamma_1)}{\acute{R}} < H(S|H), \frac{C(\gamma_2)}{\acute{R}} \geq 0 \right\}$$

$$= Pr\left\{ 0 \leq \gamma_1 < \left(2^{\acute{R}H(S|H)} - 1 \right), \gamma_2 \geq 0 \right\}$$

$$= \int_0^{2^{\acute{R}H(S|H)}-1} f_{\kappa\mu}(\gamma_1) \int_0^{\infty} f_{\kappa\mu}(\gamma_2) d\gamma_2 d\gamma_1$$

$$= \frac{\mu^{\mu-1} m^m (1+\kappa)^\mu)}{\Gamma(\mu)(\mu\kappa + m)^m} \left(\frac{1}{\bar{\gamma}_1} \right)^\mu$$

$$\times \Phi_2\left(\mu - m, m; \mu + 1; -\frac{\mu(1+\kappa)\left(2^{\acute{R}H(S|H)} - 1 \right)}{\bar{\gamma}_1}, \right.$$

$$\left. -\frac{\mu(1+\kappa)m\left(\acute{R}H(S|H) - 1 \right)}{\bar{\gamma}_1(\mu\kappa + m)} \right), \qquad (16)$$

and

$$P^{out}_{case2} = Pr\left\{ H(S|H) \leq \frac{C(\gamma_1)}{\acute{R}} \leq H(S), \frac{C(\gamma_1 + \gamma_2)}{\acute{R}} \leq H(S,H) \right\}$$

$$= Pr\left\{ \left(2^{\acute{R}H(S|H)} - 1 \right) \leq \gamma_1 \leq \left(2^{\acute{R}H(S)} - 1 \right), \right.$$

$$\left. 0 \leq \gamma_2 \leq \left(2^{\acute{R}H(S,H)} - 1 - \gamma_1 \right) \right\}$$

$$= \int_{2^{\acute{R}H(S|H)}-1}^{2^{\acute{R}H(S)}-1} f_{\kappa\mu}(\gamma_1) \int_0^{2^{\acute{R}H(S,H)}-1-\gamma_1} f_{\kappa\mu}(\gamma_2) d\gamma_2 d\gamma_1$$

$$= \int_{2^{\acute{R}H(S|H)}-1}^{2^{\acute{R}H(S)}-1} \frac{\mu^{\mu-1} m^m (1+\kappa)^\mu)}{\Gamma(\mu)(\mu\kappa + m)^m} \left(\frac{1}{\bar{\gamma}_2} \right)^\mu$$

$$\times \Phi_2\left(\mu - m, m; \mu + 1; -\frac{\mu(1+\kappa)\left(2^{\acute{R}H(S,H)} - 1 - \gamma_1 \right)}{\bar{\gamma}_2}, \right.$$

$$\left. -\frac{\mu(1+\kappa)m\left(2^{\acute{R}H(S,H)} - 1 - \gamma_1 \right)}{\bar{\gamma}_2(\mu\kappa + m)} \right)$$

$$\times \frac{\mu^{\mu} m^{m}(1+\kappa)^{\mu}}{\Gamma(\mu)\bar{\gamma}_1(\mu\kappa+m)^m}\left(\frac{\gamma_1}{\bar{\gamma}_1}\right)^{\mu-1}\exp\left(-\frac{\mu(1+\kappa)\gamma_1}{\bar{\gamma}_1}\right)$$

$$\times {}_1F_1\left(m,\mu;\frac{\mu^2\kappa(1+\kappa)\gamma_1}{(\mu\kappa+\mu)\bar{\gamma}_1}\right)d\gamma_1. \tag{17}$$

The outage probabilities in (16) and (17) can be calculated by a set of double integrals corresponding to the admissible rate region with respect to the PDFs of the instantaneous SNRs of the transmission channels, with accurate calculation error control, according to the algorithm for approximately calculating the integral over generalized rectangles and sectors [35]. The computational complexity evaluation of the analytical expressions is left as future work.

3.4 | Asymptotic tendency analyses

3.4.1 | Independent case

When S and H are completely independent, the bit flipping probability $p = 0.5$ and $H(\text{S}|\text{H}) = H(\text{H}|\text{S}) = H(\text{H}) = H(\text{S}) = 1$ based on the binary source assumption. Therefore, $\text{P}^{\text{out}}_{\text{case2}} = 0$ and hence, the outage probability is determined by $\text{P}^{\text{out}}_{\text{case1}}$ only. From (16), the H-D link has no effect on $\text{P}^{\text{out}}_{\text{case1}}$, and hence the outage probability is equivalent to that of a single S-D link transmission system without any help from H. Therefore, no diversity can be achieved in this case.

3.4.2 | Fully correlated case

When S and H are fully correlated, the bit flipping probability $p = 0$ and $H(\text{S}|\text{H}) = H(\text{H}|\text{S}) = 0$. Therefore, $\text{P}^{\text{out}}_{\text{case1}} = 0$ according to (16). In this case, the outage probability is determined only by $\text{P}^{\text{out}}_{\text{case2}}$. The second order diversity is achieved in this case, as shown in Figure 8 in Section 4.

3.4.3 | Large average SNR case

When $\bar{\gamma}_1 \to \infty$ and $\bar{\gamma}_2 \to \infty$, the value of the confluent hypergeometric function ${}_1F_1(\cdot)$ and the bivariate confluent hypergeometric function $\Phi_2(\cdot)$ in (3) and (4) reach unity, respectively. Therefore, the asymptotic behaviour of the outage probability is expressed as

$$\text{P}^{\text{out}} \sim \frac{\mu^{\mu-1} m^m (1+\kappa)^{\mu}}{\Gamma(\mu)(\mu\kappa+m)^m}\left(\frac{1}{\bar{\gamma}_1}\right)^{\mu}$$

$$+\frac{\mu^{\mu-1} m^m (1+\kappa)^{\mu}}{\Gamma(\mu)(\mu\kappa+m)^m}\left(\frac{1}{\bar{\gamma}_2}\right)^{\mu}\frac{\mu^{\mu} m^m (1+\kappa)^{\mu}}{\Gamma(\mu)\bar{\gamma}_1(\mu\kappa+m)^m}$$

$$\times\left[\bar{\gamma}_1\frac{1}{\mu^{\mu}(\kappa+1)^{\mu}}\Gamma\left(\mu,\frac{\mu(1+\kappa)\left(2^{\hat{R}H(\text{S}|\text{H})}-1\right)}{\bar{\gamma}_1}\right)\right.$$

$$\left.-\bar{\gamma}_1\frac{1}{\mu^{\mu}(\kappa+1)^{\mu}}\Gamma\left(\mu,\frac{\mu(1+\kappa)\left(2^{\hat{R}H(\text{S})}-1\right)}{\bar{\gamma}_1}\right)\right], \tag{18}$$

where $\Gamma(\cdot,\cdot)$ is the upper incomplete gamma function.

3.5 | Diversity order and coding gain

In the case of the channel variations of the S-D and H-D links following Rayleigh distributions ($\kappa = 0$ and $\mu = 1$ in shadowed κ-μ fading), by setting the geometric gain of each link to identical and replacing $\bar{\gamma}_1$ and $\bar{\gamma}_2$ with a generic $\bar{\gamma}$, corresponding to S-D and H-D links have the same distance, the outage expression reduces to

$$\text{P}^{\text{out}} = 1-\exp\left\{\cup\frac{2^{\hat{R}H(\text{S}|\text{H})}-1}{\bar{\gamma}}\right\}+\int_{2^{\hat{R}H(\text{S}|\text{H})}-1}^{2^{\hat{R}H(\text{S})}-1}\frac{1}{\bar{\gamma}}\exp\left(\cup\frac{\gamma_1}{\bar{\gamma}}\right)$$

$$\times\left[1-\exp\left(\cup\frac{2^{\hat{R}H(\text{S},\text{H})}-1-\gamma_1}{\bar{\gamma}}\right)\right\}$$

$$\approx\frac{2^{\hat{R}H(\text{S}|\text{H})}-1+\left(2^{(\hat{R}H(\text{S},\text{H})}-1\right)\left(2^{(\hat{R}H(\text{S})}-2^{(\hat{R}H(\text{S},\text{H})}-2\right)}{\bar{\gamma}^2}, \tag{19}$$

where the approximation

$$\exp(-x) = \sum_{n=0}^{\infty}\frac{(-x)^n}{n!} \approx 1-x, \tag{20}$$

has been made, as in [36], assuming high average SNR regime. With this approximation, (19) can be expressed as:

$$\text{P}^{\text{out}} = \left(G_c \times \bar{\gamma}\right)^{-G_d}, \tag{21}$$

where $G_d = 2$ and

$$G_c = \frac{1}{\sqrt{2^{\hat{R}H(\text{S}|\text{H})}-1+\left(2^{(\hat{R}H(\text{S},\text{H})}-1\right)\left(2^{(\hat{R}H(\text{S})}-2^{(\hat{R}H(\text{S},\text{H})}-2\right)}}, \tag{22}$$

are the diversity order and the coding gain[37], respectively. Since the coding gain appears in the form of the parallel shift of the outage curves and the diversity order represents the outage

curves decay, the derived outage probability in Rayleigh fading (corresponding to $\kappa = 0$ and $\mu = 1$ in shadowed κ-μ fading) serves as a design reference for practical communication system performance.

Equation (22) indicates that the coding gain depends on the total rate of the joint source-channel coding $\dot{R}$ and the correlation between the source and the helper. The generic explicit expression derivation for the diversity order and the coding gain in shadowed κ-μ fading may be challenging due to the integrals with the confluent hypergeometric functions, which is left as a future study.

3.6 | Outage derivation with CCC

In this section, we derived the outage probability of the one-source-with-one-helper transmission over MAC with CCC assumption. Since there is no closed-form expression for calculating the explicit CCC, with an approximated equation of CCC [34], the relationship between the instantaneous channel SNR γ_1 ($i \in \{1, 2\}$) and the rate $\dot{R}$ is written as

$$
\begin{cases}
\dot{R} \times H(\mathrm{S}) = C(\gamma_1) = \log_2(1 + \gamma_1) - \frac{1}{2}\log_2\left[1 + \left(\frac{\gamma_1}{M}\right)\right] \\
\dot{R} \times H(\mathrm{H}) = C(\gamma_2) = \log_2(1 + \gamma_2) - \frac{1}{2}\log_2\left[1 + \left(\frac{\gamma_2}{M}\right)\right]
\end{cases}
\tag{23}
$$

with M-ary quadrature amplitude modulation(QAM) to facilitate the outage calculation. The inverse function of (23) is written as

$$
\begin{cases}
\gamma_1 = C_{\mathrm{cc}}^{-1}[\dot{R}H(\mathrm{S})] = \dfrac{M 2^{\dot{R}H(\mathrm{S})}\sqrt{M^2 - 4^{\dot{R}H(\mathrm{S})} + 1} - M^2}{M^2 - 4^{\dot{R}H(\mathrm{S})}} \\
\gamma_2 = C_{\mathrm{cc}}^{-1}[\dot{R}H(\mathrm{H})] = \dfrac{M 2^{\dot{R}H(\mathrm{H})}\sqrt{M^2 - 4^{\dot{R}H(\mathrm{H})} + 1} - M^2}{M^2 - 4^{\dot{R}H(\mathrm{H})}}.
\end{cases}
\tag{24}
$$

Figure 7 shows that in the low SNR region the difference between GCC and CCC is very small. Whereas, in the high SNR region, the difference between GCC and CCC becomes significant. The approximated CCC has been evaluated in [34] which demonstrates that (23) is very accurate to represent CCC.

Then, the outage probability with CCC can be calculated as

$$
P_{\mathrm{case1}}^{\mathrm{out-ccc}} = \int_0^{C_{\mathrm{cc}}^{-1}[\dot{R}H(\mathrm{S}|\mathrm{H})]} f_{\kappa\mu}(\gamma_1)\int_0^\infty f_{\kappa\mu}(\gamma_2)d\gamma_2 d\gamma_1
$$

$$
= \frac{\mu^{\mu-1} m^m (1+\kappa)^\mu}{\Gamma(\mu)(\mu\kappa + m)^m}\left(\frac{1}{\bar{\gamma}_1}\right)^\mu
$$

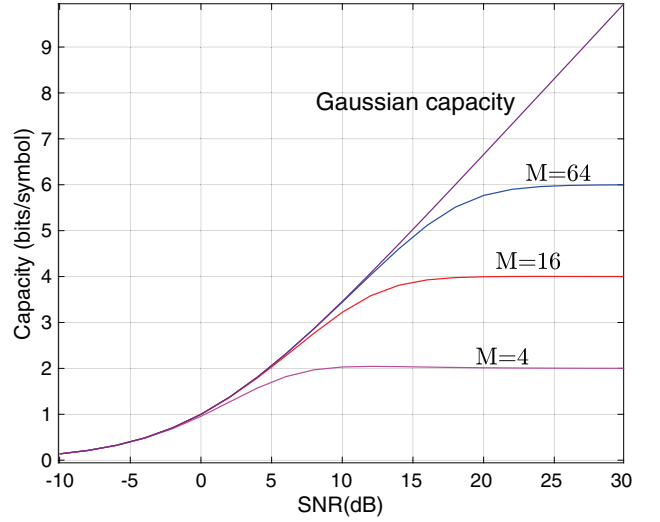**FIGURE 7** Comparison of the Gaussian codebook capacity (GCC) and constellation constrained capacity (CCC)

$$
\times \Phi_2\left(\mu - m, m; \mu + 1; -\frac{\mu(1+\kappa)\left(C_{\mathrm{cc}}^{-1}[\dot{R}H(\mathrm{S}|\mathrm{H})]\right)}{\bar{\gamma}_1},\right.
$$

$$
\left. -\frac{\mu(1+\kappa)m\left(\dot{R}H(\mathrm{S}|\mathrm{H}) - 1\right)}{\bar{\gamma}_1(\mu\kappa + m)}\right),
\tag{25}
$$

and

$$
P_{\mathrm{case2}}^{\mathrm{out-ccc}} = \int_{C_{\mathrm{cc}}^{-1}[\dot{R}H(\mathrm{S}|\mathrm{H})]}^{C_{\mathrm{cc}}^{-1}[\dot{R}H(\mathrm{S})]} f_{\kappa\mu}(\gamma_1)d\gamma_1
$$

$$
\times \int_0^{C_{\mathrm{cc}}^{-1}[\dot{R}H(\mathrm{S,H})]-\gamma_1} f_{\kappa\mu}(\gamma_2)d\gamma_2
$$

$$
= \int_{C_{\mathrm{cc}}^{-1}[\dot{R}H(\mathrm{S}|\mathrm{H})]}^{C_{\mathrm{cc}}^{-1}[\dot{R}H(\mathrm{S})]} \frac{\mu^{\mu-1} m^m (1+\kappa)^\mu}{\Gamma(\mu)(\mu\kappa + m)^m}\left(\frac{1}{\bar{\gamma}_2}\right)^\mu
$$

$$
\times \Phi_2\left(\mu - m, m; \mu + 1; \frac{-\mu(1+\kappa)\left(2^{\dot{R}H(\mathrm{S,H})} - 1 - \gamma_1\right)}{\bar{\gamma}_2}\right.
$$

$$
\left. -\frac{\mu(1+\kappa)m\left(C_{\mathrm{cc}}^{-1}[\dot{R}H(\mathrm{S,H})] - \gamma_1\right)}{\bar{\gamma}_2(\mu\kappa + m)}\right)
$$

$$
\times \frac{\mu^\mu m^m (1+\kappa)^\mu}{\Gamma(\mu)\bar{\gamma}_1(\mu\kappa + m)^m}\left(\frac{\gamma_1}{\bar{\gamma}_1}\right)^{\mu-1}\exp\left(-\frac{\mu(1+\kappa)\gamma_1}{\bar{\gamma}_1}\right)
$$

$$
\times {}_1\mathrm{F}_1\left(m, \mu; \frac{\mu^2\kappa(1+\kappa)\gamma_1}{(\mu\kappa + \mu)\bar{\gamma}_1}\right)d\gamma_1.
\tag{26}
$$

Note that the theoretical derivation of outage probability is based on the modified Slepian–Wolf region and the MAC region, and presumed infinite frame length, which results in the derived outage probabilities being the upper bounds of the practical numerical results. Therefore, the derived outage probability can serve as a reference limit in practical coding/decoding design for transmitting one source with one helper over a fading MAC.

3.7 | Optimal power allocation analyses

In this subsection, the total transmit power of the system is assumed to be fixed as $\acute{P}$. Then, we have

$$
\begin{cases}
P_1 + P_2 = \acute{P} \\
P_1/\acute{P} = \alpha \\
P_2/\acute{P} = 1 - \alpha
\end{cases}, \tag{27}
$$

where the P_1 and P_2 are the average transmit powers for S and H, respectively, and α is the ratio of the transmit power allocated for S, and the value is kept constant within a block duration, under the block fading assumption.

The optimization problem with regard to α can be formulated as

$$
\begin{aligned}
\alpha^* &= \arg\min_{k} \quad P_{\text{out}}(\alpha) \\
&\text{subject to:} \quad \alpha \in (0, 1).
\end{aligned} \tag{28}
$$

This section aims to find the optimal α^* that minimizes the outage probability. By the normalized noise variance of the both channels to the unity, the outage probability expressions in (16) and (17) are rewritten as

$$
P_{\text{case1}}^{\text{out}} = \frac{\mu^{\mu-1} m^m (1+\kappa)^\mu}{\Gamma(\mu)(\mu\kappa+m)^m} \left(\frac{1}{\alpha\acute{P}}\right)^\mu
$$
$$
\times \Phi_2\left(\mu-m, m; \mu+1; -\frac{\mu(1+\kappa)\left(2^{\acute{R}H(\text{S}|\text{H})}-1\right)}{\alpha\acute{P}} \right.
$$
$$
\left. -\frac{\mu(1+\kappa)m\left(\acute{R}H(\text{S}|\text{H})-1\right)}{\alpha\acute{P}(\mu\kappa+m)} \right), \tag{29}
$$

and

$$
P_{\text{case2}}^{\text{out}} = \int_{2^{\acute{R}H(\text{S}|\text{H})}-1}^{2^{\acute{R}H(\text{S})}-1} \frac{\mu^{\mu-1} m^m (1+\kappa)^\mu}{\Gamma(\mu)(\mu\kappa+m)^m} \left(\frac{1}{(1-\alpha)\acute{P}}\right)^\mu
$$
$$
\times \Phi_2\left(\mu-m, m; \mu+1; -\frac{\mu(1+\kappa)\left(2^{\acute{R}H(\text{S},\text{H})}-1-\gamma_1\right)}{(1-\alpha)\acute{P}} \right.
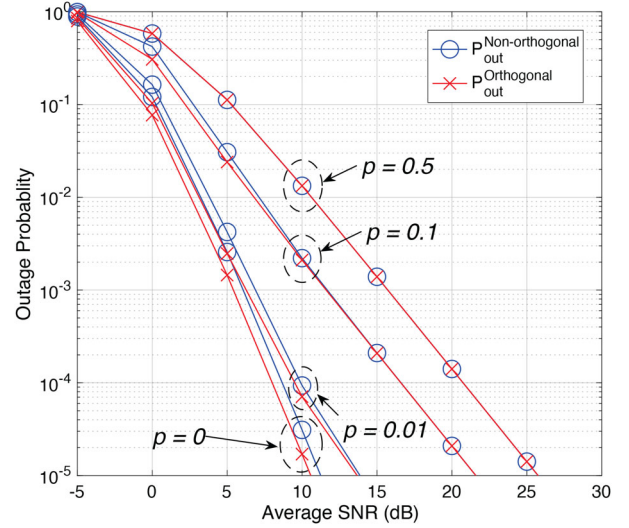$$

FIGURE 8 Comparison between the outage probabilities of orthogonal and non-orthogonal transmission. $\bar{\gamma}_1 = \bar{\gamma}_2$, $m_1 = m_2 = 3$, $\kappa_1 = \kappa_2 = 2$, and $\mu_1 = \mu_2 = 2$

$$
\left. -\frac{\mu(1+\kappa)m\left(2^{\acute{R}H(\text{S},\text{H})}-1-\gamma_1\right)}{(1-\alpha)\acute{P}(\mu\kappa+m)} \right)
$$
$$
\times \frac{\mu^\mu m^m (1+\kappa)^\mu}{\Gamma(\mu)\bar{\gamma}_1(\mu\kappa+m)^m} \left(\frac{\gamma_1}{\alpha\acute{P}}\right)^{\mu-1} \exp\left(-\frac{\mu(1+\kappa)\gamma_1}{\alpha\acute{P}}\right)
$$
$$
\times {}_1\text{F}_1\left(m, \mu; \frac{\mu^2\kappa(1+\kappa)\gamma_1}{(\mu\kappa+\mu)\alpha\acute{P}} \right) d\gamma_1, \tag{30}
$$

which are used to determine the effect of the power allocation ratio α on the outage performance. Due to the existence of the confluent hypergeometric function $\Phi_2(\cdot)$ in (29) and the bivariate confluent hypergeometric function ${}_1\text{F}_1(\cdot)$ in (30), the generic closed-form expressions derivation for the optimal power allocation problem may be challenging and the convexity of the expressions (29) and (30) is difficult to prove. Therefore, the analytical results of the optimal power allocation problem are obtained numerically and provided in the next section.

4 | NUMERICAL RESULTS

In this section, we present the numerical results to verify the accuracy of the outage probability upper bound. We assume half-rate memory-1 code and binary phase shift keying (BPSK) in the transmission. Therefore, the total joint coding rate $\acute{R}$ is set as $\acute{R} = 0.5$.

Figure 8 shows the theoretical outage probability against the average SNR with the parameter p varying from 0 to 0.5. The outage probability of correlated sources transmission over orthogonal channels [27] are presented as benchmark schemes. The average SNRs of the S-D and H-D links are assumed to be the same. We observe from the outage curves that orthogonal transmission outperforms its non-orthogonal counterpart
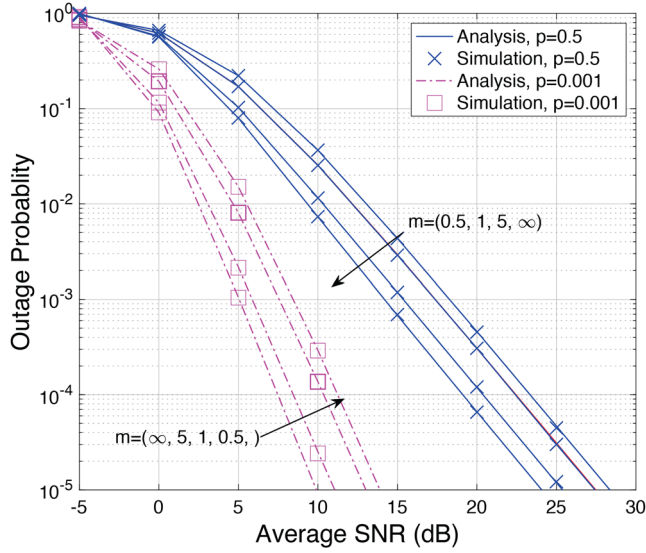
FIGURE 9 Outage probability versus average SNR with parameter $m = m_1 = m_2$. $\kappa_1 = \kappa_2 = 1.5$, and $\mu_1 = \mu_2 = 2$

FIGURE 10 Comparison of outage probabilities of analytical results and asymptotic results where $\overline{\gamma}_1 = \overline{\gamma}_2$, $\kappa_1 = \kappa_2 = 1$, $\mu_1 = \mu_2 = 1.5$, and $m_1 = m_2 = 2$

when S and H are highly correlated (small p). This indicates that the correlation between S and H is exploited at the destination. In contrast, when the correlation between S and H decreases (larger p), the advantage of orthogonal transmission over non-orthogonal transmission concerning the outage performance disappears. However, with the same p, the same diversity gain can be observed in the outage curves with either orthogonal or non-orthogonal transmission.

Figure 9 plots the outage probabilities with different shadowing parameters $m_1 (= m_2)$. The shadowing parameter value significantly affects the outage performance, both in the highly correlated case ($p = 0.001$) and the independent case ($p = 0.5$). However, the decline in the outage curves (equivalent to diversity gain) is not affected by the value of shadowing parameter $m_1 (= m_2)$. Figure 9 also shows that the Monte Carlo simulation results are in excellent agreement with the analytical derivations. The simulations for the integrals in (16) and (17) are implemented by evaluating the integral function with a large number of shadowed κ-μ distributed random points and averaging.

Figure 10 shows the outage curves of analytical results based on (16) and (17) and asymptotic results based on (18). We infer from these results that the asymptotic outage behaviour and the analytical results are in good agreement in the high SNR region. It is also found from Figure 10 that in the multipath clusters case ($\mu > 1$), more than second-order diversity is achieved when the information sequences between S and D are fully correlated ($p = 0$).

Figures 11 and 12 compare the outage probabilities in (16) and (17) derived with GCC, and those in (25) and (26) derived with CCC. The total coding efficiency $\acute{R}$ is set as $\acute{R} = 0.5$ in Figure 11 and $\acute{R} = 5$ in Figure 12. It is found that, the difference between the GCC based and the CCC based outage performance is negligible in Figure 11. This is because the smaller value of $\acute{R}$ (equivalent to lower spectrum efficiency or lower source rate) results in lower outage probability. Therefore, the
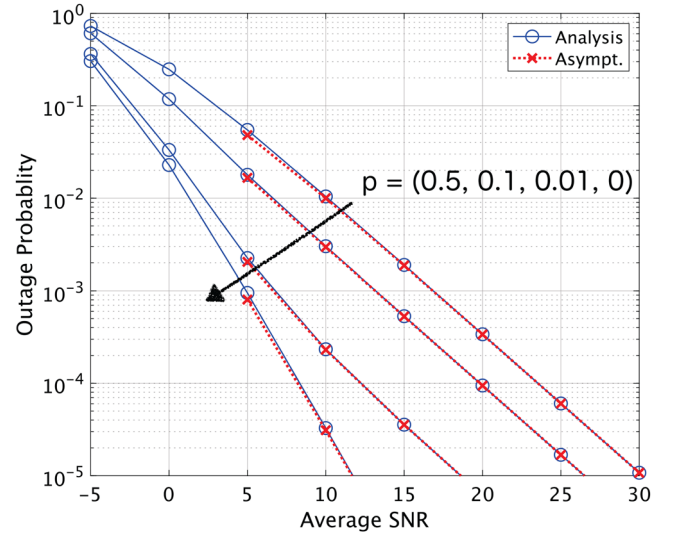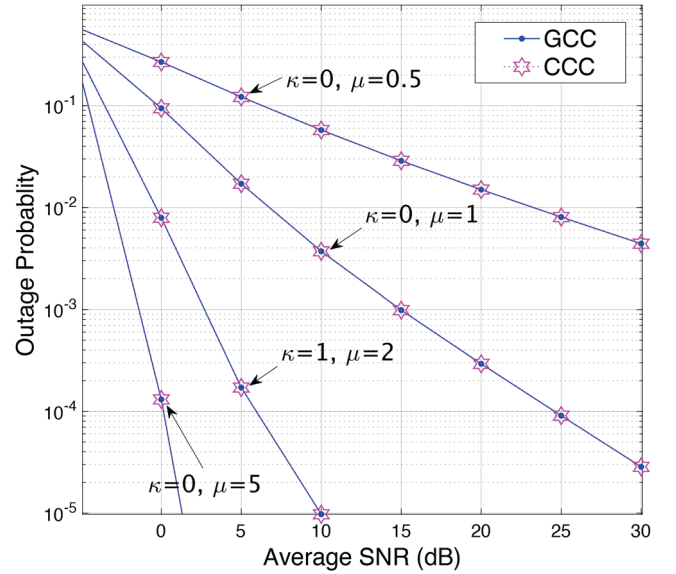

FIGURE 11 Comparison of the outage probability with GCC and CCC. $\acute{R} = 0.5$, $p = 0.01$, $\overline{\gamma}_1 = \overline{\gamma}_2$, $m = m_1 = m_2 = \infty$, $\kappa = \kappa_1 = \kappa_2$, and $\mu = \mu_1 = \mu_2$

effect of the differences between GCC and CCC on the outage probability is negligibly small. In contrast, when the value of $\acute{R}$ is larger (equivalent to higher spectrum efficiency or higher source rate), which results in higher outage probability, the significant difference can be observed between the GCC and CCC based outage performances as shown in Figure 12, especially in the high SNR region. This result is consistent with the capacity tendency shown in Figure 7.

Figure 13 illustrates the outage performance curves versus the power allocation ratio α with different flipping probability p. The x-axis indicates the ratio α of the transmit power allocated to S. The total transmit power is set at 10 dB with the noise
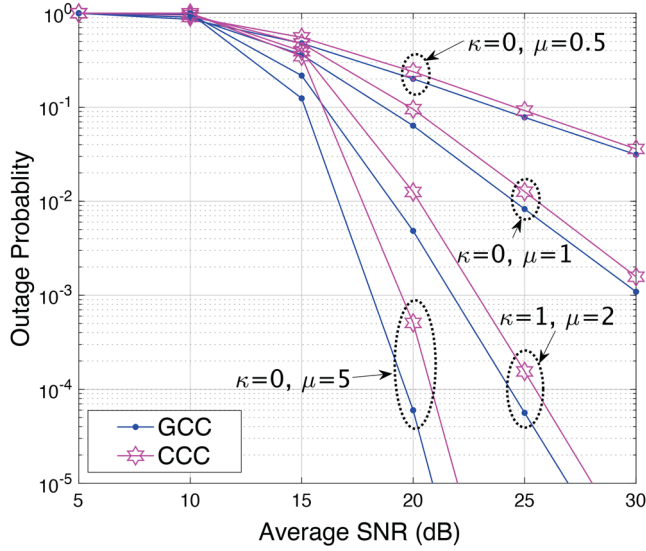
FIGURE 12 Comparison of the outage probability with GCC and CCC. $\dot{R} = 5$, $p = 0.01$, $\overline{\gamma}_1 = \overline{\gamma}_2$, $m = m_1 = m_2 = \infty$, $\kappa = \kappa_1 = \kappa_2$, and $\mu = \mu_1 = \mu_2$
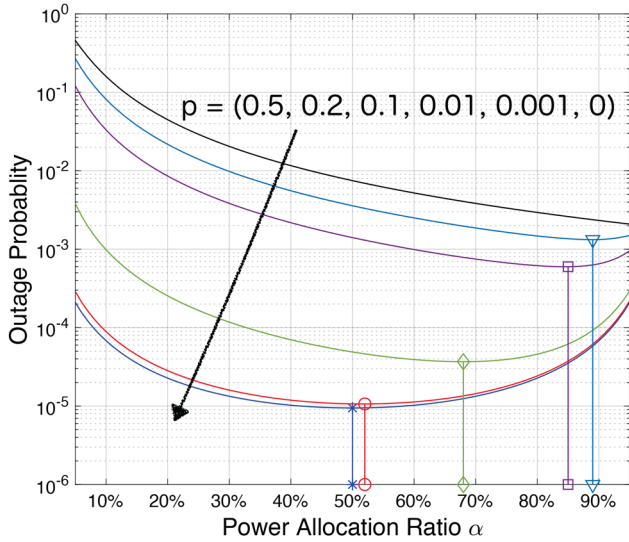

FIGURE 14 Optimal power allocation for minimizing the outage probability with different κ_2, where $\overline{\gamma}_1 = \overline{\gamma}_2$, $\kappa_1 = 1$, $\mu_1 = \mu_2 = 1$, and $p = 0.001$

FIGURE 13 Optimal power allocation for minimizing the outage probability with different p, where $\overline{\gamma}_1 = \overline{\gamma}_2$, $\kappa_1 = \kappa_2 = 1$, and $\mu_1 = \mu_2 = 2$

variation being normalized to the unity. The computational granularity for the optimal power allocation is 1% of α in the numerical calculation. We understand from Figure 13 that if the information sequences of S and H are fully correlated ($p = 0$), the lowest outage probability can be achieved when the transmit power is equally allocated to both S and H. It can also be found that the optimal ratio α achieving the minimum outage probability becomes large, as the value of p increases. This is reasonable because when the help provided by H becomes less useful we should assign more power to S. When S and H are independent ($p = 0.5$), all the transmit power should be assigned to S.

Figure 14 shows the outage probability versus the power allocation ratio α, with κ_2 as a parameter. We find that the optimal
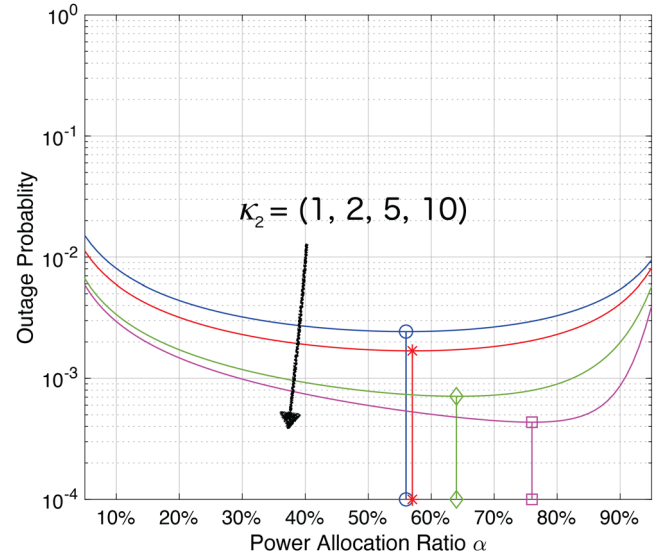
α, that achieves the smallest outage probability increases with increasing κ_2 value. This indicates that a large dominant component power ratio in H-D channel expands the effects of errors, since S and H are not fully correlated (S $\neq$ H with probability $p = 0.001$). Namely, assigning more power to H can not help to improve the outage performance. In contrast, in this case, it is more effective to assign more power to S other than to H.

5 | CONCLUSIONS

In this study, we have analysed the outage probability of the one-source-with-one-helper transmission over block shadowed κ-μ fading MAC. The exact expression for the outage probability upper bound has been derived, and the closed-form outage expression has also been obtained through a reasonable high-SNR approximation. We have found that the difference between the CCC-based outage probability and the GCC-based outage probability is very minor with low spectrum efficiency or source rate. In contrast, such difference become significant when the spectrum efficiency or source rate becomes high. It has also been found that the outage performance of the orthogonal transmission is superior compared to its non-orthogonal counterpart with high correlation between the source and the helper. Shadowing affects the outage performance significantly, regardless of the correlation between the source and the helper; however, the shadowing does not affect the diversity gain, as shown in the outage curves. The accuracy of the analytical results has been verified by a series of Monte Carlo simulations. The optimal power allocation has also been analysed with fixed total power. The analytical results indicate that the lower outage probability can not always be achieved by increasing the ratio of power allocated to the helper, even if the ratio of the dominant component in the helper-destination channel is high.

Since the lossless coding is not always a mandatory requirement in some decision-making systems, and the distortion is accepted with a specific distortion level as a quality-of-service requirement, the rate-distortion and outage probability analyses for Wyner-Ziv systems are promising research topics for our further study.

ACKNOWLEDGEMENTS

CONFLICT OF INTEREST

The authors declare no conflicts of interest associated with this manuscript.

PERMISSION TO REPRODUCE MATERIALS FROM OTHER SOURCES

None

DATA AVAILABILITY STATEMENT

Data sharing not applicable—the article describes entirely theoretical research.

ORCID

Shen Qian https://orcid.org/0000-0002-2704-9109

REFERENCES

1. Shin, S., Kwon, T.: A privacy-preserving authentication, authorization, and key agreement scheme for wireless sensor networks in 5G-integrated internet of things. IEEE Access 8, 67555–67571 (2020)
2. Bourdoux, A, Barreto, A.N., v Liempd, B., et al.: 6G white paper on localization and sensing. arXiv:200601779 [eessSY] (2020)
3. Ciuonzoand, D., Rossi, P.S.: Data Fusion in Wireless Sensor Networks: A Statistical Signal Processing Perspective. IET, London (2019)
4. Matsuta, T., Uyematsu, T.: Coding theorems for asynchronous Slepian-Wolf coding systems. IEEE Trans. Inform. Theory 66(8), 4774–4795 (2020)
5. Cover, T.M., Thomas, J.A.: Elements of Information Theory, 2nd ed. John Wiley & Sons, Inc., Hoboken (2006)
6. Wan, D., Wen, M., Ji, F., Yu, H., Chen, F.: Non-orthogonal multiple access for cooperative communications: Challenges, opportunities, and trends. IEEE Wireless Commun. Mag. 25(2), 109–117 (2018)
7. He, J., Hussain, I., Juntti, M., et al.: End-to-end outage probability analysis for multi-source multi-relay systems. In: Proceedings of IEEE International Conference on Communications, pp. 1–6. IEEE, Piscataway (2016)
8. Bross, S.I., Laufer, Y.: Sending a bivariate gaussian source over a gaussian mac with unidirectional conferencing encoders. IEEE Trans. Inform. Theory 62(3), 1296–1311 (2016)
9. Padakandla, A.: Communicating correlated sources over MAC and interference channels I: Separation-based schemes. IEEE Trans. Inform. Theory 66(7), 4104–4128 (2020)
10. Padakandla, A.: Communicating correlated sources over MAC and interference channels II: Joint source-channel coding. IEEE Trans. Inform. Theory 67(6), 3847–3872 (2021)
11. Zhou, X., He, X., Juntti, M., et al.: Outage probability of correlated binary source transmission over fading multiple access channels. In: Proceedings of IEEE Workshop on Signal Processing Advances in Wireless Communications, pp. 96–100. IEEE, Piscataway (2015)
12. He, J., Tervo, V., Qian, S., et al.: Performance analysis of lossy decode-and-forward for non-orthogonal MARCs. IEEE Trans. Wireless Commun. 17(3), 1545–1558 (2018)
13. Song, S., Cheng, M., He, J., et al.: Outage probability of one-source-with-one-helper sensor systems in block rayleigh fading multiple access channels. IEEE Sensors J. 21(2), 2140–2148 (2021)
14. Song, S., He, J., Matsumoto, T.: Rate-distortion and outage probability analyses of wyner-ziv systems over multiple access channels. IEEE Trans. Commun. 69(9), 5807–5816 (2021)
15. Cotton, S.L.: Human body shadowing in cellular device-to-device communications: Channel modeling using the shadowed κ-μ fading model. IEEE J. Select Areas Commun. 33(1), 111–119 (2015)
16. Zeng, J., Lv, T., Liu, R.P., Su, X., Guo, Y.J., Beaulieu, N.C.: Enabling ultra-reliable and low-latency communications under shadow fading by massive MU-MIMO. IEEE Internet Things J. 7(1), 234–246 (2020)
17. Paris, J.F.: Statistical characterization of κ-μ shadowed fading. IEEE Trans. Veh. Technol. 63(2), 518–526 (2014)
18. Yacoub, M.D.: The κ-μ distribution and the η-μ distribution. IEEE Antennas Propagat. Mag. 49(1), 68–81 (2007)
19. Chun, Y.J., Cotton, S.L., Dhillon, H.S., et al.: A comprehensive analysis of 5G heterogeneous cellular systems operating over κ-μ shadowed fading channels. IEEE Trans. Wireless Commun. 16(11), 6995–7010 (2017)
20. Kumar, S., Kalyani, S.: Outage probability and rate for κ-μ shadowed fading in interference limited scenario. IEEE Trans. Wireless Commun. 16(12), 8289–8304 (2017)
21. Bhatnagar, M.R.: On the sum of correlated squared $\kappa - \mu$ shadowed random variables and its application to performance analysis of mrc. IEEE Trans. Veh. Technol. 64(6), 2678–2684 (2015)
22. Zhang, J., Chen, X., Peppas, K.P., Li, X., Liu, Y.: On high-order capacity statistics of spectrum aggregation systems over κ - μ and κ - μ shadowed fading channels. IEEE Trans. Commun. 65(2), 935–944 (2017)
23. Li, X., Li, J., Li, L., Jin, J., Zhang, J., Zhang, D.: Effective rate of miso systems over κ - μ shadowed fading channels. IEEE Access 5, 10605–10611 (2017)
24. ElHalawany, B.M., Jameel, F., da Costa, D.B., Dias, U.S., Wu, K.: Performance analysis of downlink noma systems over κ-μ shadowed fading channels. IEEE Trans. Veh. Technol. 69(1), 1046–1050 (2020)
25. Yang, J., Wu, X., Peppas, K.P., Mathiopoulos, P.T.: Capacity analysis of power beacon-assisted energy harvesting MIMO system over $\kappa - \mu$ shadowed fading channels. IEEE Trans. Veh. Technol. 70(11), 11869–11880 (2021)
26. Liu, S., Wang, J., Bao, J., et al.: Optimized SCMA codebook design by QAM constellation segmentation with maximized MED. IEEE Access 6, 63232–63242 (2018)
27. Qian, S., Zhou, X., He, X., et al.: Performance analysis for lossy-forward relaying over Nakagami-*m* fading channels. IEEE Trans. Veh. Technol. 66(11), 10035–10043 (2017)
28. He, J., Tervo, V., Zhou, X., He, X., Qian, S., Cheng, M., et al.: A tutorial on lossy forwarding cooperative relaying. IEEE Commun. Surv. Tutorials 21(1), 66–87 (2019)
29. Moreno-Pozas, L., Lopez-Martinez, F.J., Paris, J.F., et al.: The κ-μ shadowed fading model: Unifying the κ-μ and η-μ distributions. IEEE Trans. Veh. Technol. 65(12), 9630–9641 (2016)
30. Gradshteyn, I.S., Ryzhik, I.M.: Table of Integrals, Series, and Products, Eighth edn. Academic Press, Cambridge (2014)
31. Lopez-Martinez, F.J., Paris, J.F., Romero-Jerez, J.M.: The κ-μ shadowed fading model with integer fading parameters. IEEE Trans. Veh. Technol. 66(9), 7653–7662 (2017)
32. Garcia-Frias, J., Zhao, Y.: Near-Shannon/Slepian-Wolf performance for unknown correlated sources over AWGN channels. IEEE Trans. Commun. 53(4), 555–559 (2005)
33. Zhou, X., Cheng, M., He, X., et al.: Exact and approximated outage probability analyses for decode-and-forward relaying system allowing intra-link errors. IEEE Trans. Wireless Commun. 13(12), 7062–7071 (2014)

34. Cheng, M., Lin, W., Matsumoto, T.: Down-link NOMA with successive refinement for binary symmetric source transmission. IEEE Trans. Commun. 68(12), 7927–7937 (2020)

35. Shampine, L.F.: Matlab program for quadrature in 2D. EURASIP J Appl. Math. Comput. 202(1), 266–274 (2008)

36. Qian, S., He, J., Juntti, M., et al.: Fading correlations for wireless cooperative communications: Diversity and coding gains. IEEE Access 5, 8001–8016 (2017)

37. Wang, Z., Giannakis, G.B.: A simple and general parameterization quantifying performance in fading channels. IEEE Trans. Commun. 51(8), 1389–1398 (2003)